The 9th European Congress on Computational Methods in Applied Sciences and Engineering
ECCOMAS Congress 2024
3–7 June 2024, Lisboa, Portugal

# OPTIMIZATION OF GEOMETRY FOR TURBULENT FLOW USING THE CONTINUOUS ADJOINT METHOD

**Carlos J. Ruiz[1,*], A. Martínez-Cava[1,2], M. Chávez-Modena[1,3] and E. Valero[1,3]**

[1] Universidad Politécnica de Madrid, Plaza Cardenal Cisneros 3, E-28040 Madrid, Spain

[2] Instituto Universitario "Ignacio Da Riva" (IDR/UPM), Universidad Politécnica de Madrid, Plaza Cardenal Cisneros, 3, E-28040, Madrid, Spain

[3] CCS-UPM - Centre for Computational Simulation, Universidad Politécnica de Madrid, Boadilla del Monte, E-28660, Madrid, Spain

**Key words:** Turbulent flow, Sensitivity analysis, Adjoint methods, Finite Elements, FEniCSx

**Summary.** This research explores the application of the adjoint method for optimizing geometry in turbulent flows. Turbulent flows present significant challenges in computational fluid dynamics (CFD), often requiring computationally expensive simulations for accurate predictions. The adjoint method offers an efficient approach by providing sensitivity information crucial for optimization. This study investigates the integration of the adjoint method with turbulent flow simulations, specifically employing the Spalart-Allmaras model in a Venturi-type pipe, to optimize geometry for specific performance objectives.

## 1 Introduction

Geometry optimization is a cornerstone of modern fluid mechanics, with applications that significantly enhance aerodynamic performance in vehicles and boost efficiency in industrial processes. The main methods used in geometry optimization include parameterization, the adjoint method, artificial intelligence techniques, and genetic algorithms.

Artificial intelligence techniques [1], such as machine learning and neural networks, are used to model complex systems and predict optimal solutions. These methods handle large data sets and uncover patterns that traditional optimization methods might miss. Parameterization involves defining a set of parameters that describe the geometry or system to be optimized [2]. Using a systematic variation of these parameters, optimal configurations can be identified that meet the desired performance criteria. Genetic algorithms, [3], inspired by natural selection, evolve a population of candidate solutions through selection, crossover, and mutation operations to identify the best-performing individuals. Both parameterization and genetic algorithms are computationally intensive, with a tendency to converge slowly or become trapped in local minima, often leading to suboptimal solutions. The adjoint method is used to efficiently compute the gradient of a performance measure with respect to design variables, guiding the optimization process, particularly useful in fluid dynamics and other continuous systems. In this work, we have opted for the adjoint method, as it allows us to derive physical insights from the governing equations of the problem's dynamics.

The first time in history that adjoint equations were used for design was in 1970 by [4], but it was not until 1988, [5, 6], that the first applications were made in the field of computational fluid dynamics (CFD). From this point on, CFD codes for optimization began to be developed, [7, 8]. For a comprehensive review of these early algorithms, refer to [9], and for an introductory look at the field, see [10].

Adjoint methods have transformed optimization in fluid mechanics by enabling efficient sensitivity analysis. They compute the gradient of an objective function with respect to numerous design variables within a single simulation, using equations derived directly from the governing flow dynamics [11]. This significantly reduces computational costs compared to traditional methods that require multiple direct simulations. Adjoint methods offer accurate gradient information essential for guiding the optimization process toward the optimal solution.

Understanding the distinctions between continuous and discrete adjoint methods is crucial for selecting the appropriate technique for a given optimization problem. The continuous adjoint method involves deriving adjoint equations in a continuous form before discretizing them for numerical solutions, ensuring consistency with the continuous governing equations, [11, 12]. On the other hand, the discrete adjoint method first discretizes the governing flow equations, and then derives adjoint equations from the discrete system, ensuring consistency with the numerical scheme used for the direct problem, [13, 14].

Due to the fact that many aerodynamic problems are studied under turbulent conditions, it is essential to develop methodologies specifically tailored for these regimes. Examples of studies using the continuous adjoint method for turbulent flows can be found in [15, 16, 17] for Spalart-Allmaras model or [18] for $k-\omega$ model. These optimization methods often require pre-calculation of gradients, which can be computationally intensive and time-consuming.

In turbulent models, certain terms depend on the distance from a point to the boundary, complicating equations and increasing computational complexity. The proposed methodology aims to simplify these terms and focus on essential sensitivities, making the optimization process more manageable and efficient. Additionally, the proposed continuous adjoint method is designed to be generalizable to unsteady cases, ensuring its applicability to a wider range of practical problems, opening a new line of study for more complex phenomena.

The development of a new continuous adjoint method for geometry optimization is driven by the need to overcome the limitations of existing approaches and address the distinct challenges of turbulent and unstable flows. This novel methodology is poised to significantly increase efficiency, accuracy, and versatility in optimization techniques.

This study is based on a previous work [19] where we derived the sensitivity for unsteady laminar flows. Our specific aim is to develop a robust formulation applicable to turbulent flows and validate this formulation with the optimization of the pressure drop in a Venturi device.

## 2 Theoretical Framework

Optimization problems can be classified as either unconstrained or constrained. On the one hand, the goal of an unconstrained optimization problem is to find the state of the system, $\mathbf{q}$, that minimizes or maximizes a scalar of the system, the cost function, $\mathcal{J}$. We assume that $\mathcal{J}$ belongs $C_1$ class, with a particular value of $\mathbf{q}$ that cancels the gradient, $\mathrm{d}\mathcal{J}/\mathrm{d}\mathbf{q}$. In most cases, this cancelation is impossible, and we can only act on a set of control parameters, $\mathbf{g}$. On the other hand, the goal of constrained optimization is to minimize or maximize the cost function,

$\mathcal{J}$, by acting on $\mathbf{g}$, where $\mathbf{q}$ and $\mathbf{g}$ are subject to $\mathbf{F}(\mathbf{q}, \mathbf{g}) = 0$.

In addition, we have to make a distinction between stationary and nonstationary problems, since the parameter to optimize does not have to depend on time, we have to integrate with respect to it and add another constraint that imposes the initial conditions.

### 2.1 Steady case

To calculate the sensitivity (the gradient) of the cost function, we introduce the Lagrangian functional as:

$$\mathcal{L}(\mathbf{q}, \mathbf{g}, \lambda) = \mathcal{J} - \lambda \cdot \mathbf{F}(\mathbf{q}, \mathbf{g}), \tag{1}$$

where $\lambda$ is the adjoint variable. A variation of the Lagrangian follows the expression:

$$\delta\mathcal{L} = \frac{\partial \mathcal{L}}{\partial \mathbf{q}}\delta\mathbf{q} + \frac{\partial \mathcal{L}}{\partial \mathbf{g}}\delta\mathbf{g} + \frac{\partial \mathcal{L}}{\partial \lambda}\delta\lambda. \tag{2}$$

The extreme condition is enforced on, since the Langrangian reaches an extremum if $\delta\mathcal{L} = 0$ for all variations, therefore the following conditions on the derivatives are imposed:

$$\frac{\partial \mathcal{L}}{\partial \mathbf{q}} = \mathbf{0}, \frac{\partial \mathcal{L}}{\partial \mathbf{g}} = \mathbf{0}, \frac{\partial \mathcal{L}}{\partial \lambda} = \mathbf{0}. \tag{3}$$

Developing these derivatives from Equation (1), we obtain the following expressions:

$$\nabla_{\mathbf{q}}\mathcal{L} := \frac{\partial \mathcal{L}}{\partial \mathbf{q}} = \frac{\partial \mathbf{F}}{\partial \mathbf{q}}^T \lambda - \frac{\partial \mathcal{J}}{\partial \mathbf{q}} = \mathbf{0}, \tag{4}$$

$$\nabla_{\mathbf{g}}\mathcal{L} := \frac{\partial \mathcal{L}}{\partial \mathbf{g}} = \frac{\partial \mathbf{F}}{\partial \mathbf{g}}\lambda - \frac{\partial \mathcal{J}}{\partial \mathbf{g}} = \mathbf{0}, \tag{5}$$

$$\nabla_{\lambda}\mathcal{L} := \frac{\partial \mathcal{L}}{\partial \lambda} = -\mathbf{F} = \mathbf{0}. \tag{6}$$

Equation (4) is so called the adjoint equation, Equation (5) is the optimization equation over $\mathbf{g}$, and the Equation (6) recovers the state equation of the model.

### 2.2 Unsteady case

Unlike the steady case, in the unsteady case the state equation depends on time,

$$\mathbf{F}(\mathbf{q}(t), \mathbf{g}, t) = \frac{\mathrm{d}\mathbf{q}}{\mathrm{d}t} - \mathbf{N}(\mathbf{q}, \mathbf{g}, t) = \mathbf{0}, \tag{7}$$

with a initial condition $\mathbf{F_0}(\mathbf{q}, \mathbf{g}, t_0) = \mathbf{q}(t_0) - \mathbf{q}_0 = \mathbf{0}$, where $\mathbf{N}$ includes the terms that do not involve a time derivative.

The Lagrangian can be defined as:

$$\mathcal{L} = \mathcal{J} - \int_{t_0}^{T} (\lambda \cdot \mathbf{F}) dt - \mu \cdot \mathbf{F}_0. \tag{8}$$

where $\lambda$, $\mu$ are the adjoint variables and $T$ corresponds to the temporal window.

The optimization system is derived by setting to zero the variation of the Lagrangian with respect to all variables, like the steady case, recovering the optimization system.

## 3 Methodology

### 3.1 Description of the problem

To validate the methodology, we consider a two-dimensional venturi device, as depicted inFigure 1.

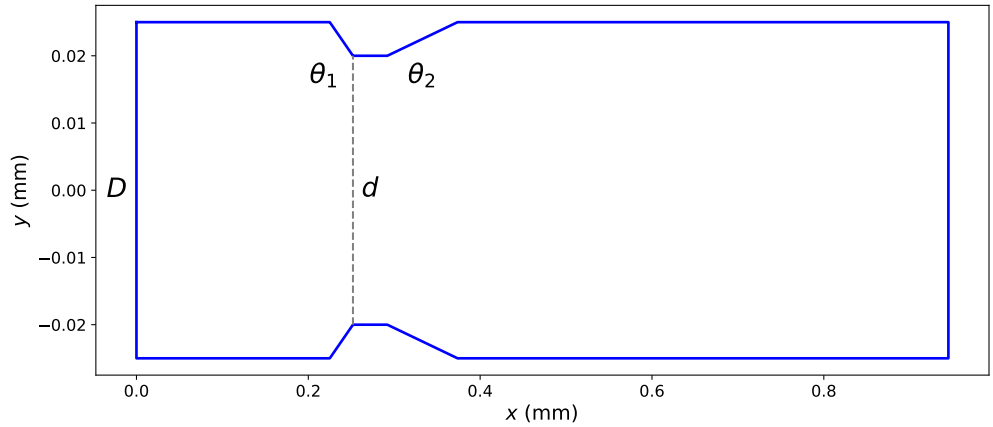


Figure 1: Sketch of the venturi device.

A Venturi device, or Venturi tube, utilizes Bernoulli's principle to measure fluid flow. It has three main sections: a converging inlet, a narrow throat, and a diverging outlet. As fluid flows through the device, its velocity increases and pressure decreases in the throat. This principle is used for applications such as flow measurement, aeration, mixing, and fuel delivery systems. The Venturi device is valued for its accuracy and simplicity in various industrial and scientific uses.

The Venturi device has specific dimensions that are crucial for its operation. In the analysis presented here the ratio of the diameter of the throat ($d$) to the diameter of the inlet ($D$) is $\beta = d/D = 0.8$. Furthermore, the convergence angle ($\theta_1$) of the Venturi is $21^{\text{o}}$. This angle defines the tapering of the inlet section as it narrows down to the throat, influencing the acceleration of the fluid entering the throat. The divergence angle ($\theta_2$) set to $7^{\text{o}}$, which describes the gradual expansion of the device after the throat.

### 3.2 Mesh Generation and Structure

The structured mesh was generated using Gmsh and carefully designed to balance computational cost and the need for precision in key areas of interest. In Figure 2, the velocity profile is depicted in three critical sections of the device: before contraction, in the throat of contraction, and after expansion. These profiles are presented for different numbers of mesh-generating points, illustrating how the resolution of the mesh affects the accuracy and detail of the simulated flow. The figure also illustrates the convergence of the solution and an intermediate mesh has been selected for the simulations.

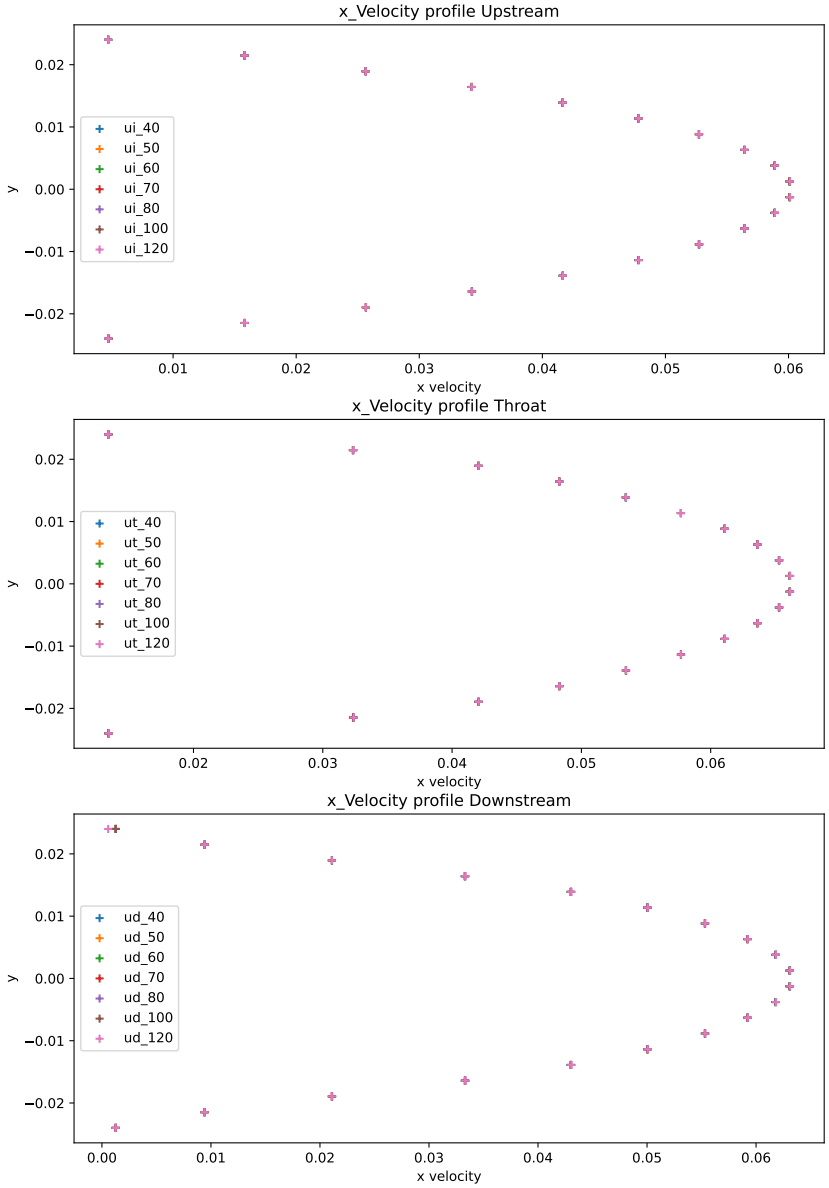


Figure 2: Velocity profiles at three sections of the device—before the contraction, at the throat, and after the expansion—for different values of the mesh generation parameter $n$. The parameter $n$ indicates the number of points used to generate the mesh.

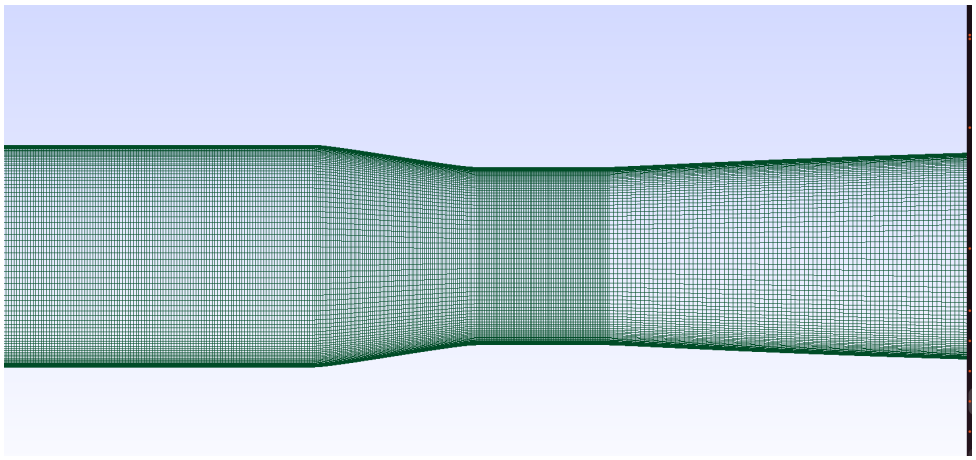

Figure 3: Computational mesh with 186290 elements.

### 3.3 Mathematical model

The fluid density, $\rho$, and the kinematic viscosity, $\nu$, are assumed constant; therefore, the non-dimensional parameter for this problem is the Reynolds number, $\mathrm{Re} = \frac{u_\infty D}{\nu}$, where $u_\infty$ is the free-stream velocity. The evolution of the fluid is ensured by the Navier-Stokes and Spalart-Allmaras equation for imcompressble flow:

$$\frac{\partial \mathbf{u}}{\partial t} + (\mathbf{u}\cdot\nabla)\mathbf{u} = -\nabla p + \nabla\cdot((\nu+\nu_t)\nabla\mathbf{u}) + \mathbf{f}, \tag{9}$$

$$\nabla\cdot\mathbf{u} = 0, \tag{10}$$

$$SA = \frac{\partial\tilde{\nu}}{\partial t} + \mathbf{u}\cdot\nabla\tilde{\nu} - C_{b1}\tilde{S}\tilde{\nu} + \frac{1}{\sigma}\left[\nabla\cdot((\nu+\tilde{\nu})\nabla\tilde{\nu}) + C_{b2}|\nabla\tilde{\nu}|^2\right] - C_{w1}f_w\left(\frac{\tilde{\nu}}{d}\right)^2 = 0, \tag{11}$$

where $\mathbf{u}$ represents the velocity vector, while $p$ denotes the pressure. The kinematic viscosity of the fluid is given by $\nu$, and $\tilde{\nu}$ is the eddy viscosity. The turbulent viscosity is defined as $\nu_t = \tilde{\nu} f_{v1}$. The modified magnitude of the vorticity is $\tilde{S} = \Omega + \frac{\tilde{\nu}}{\kappa^2 d^2} f_{v2}$, where $\Omega = \sqrt{2\Omega_{ij}\Omega_{ij}}$ is the magnitude of the vorticity, and $\Omega_{ij} = \frac{1}{2}\left(\frac{\partial u_i}{\partial x_j} - \frac{\partial u_j}{\partial x_i}\right)$ is the vorticity tensor. The variable $d$ represents the distance to the nearest wall. Model constants include $C_{b1}, C_{b2}, C_{w1}, C_{w2}, C_{w3}, \sigma, \kappa$, and $C_{v1}$, [20]. Additionally, $\mathbf{f}$ signifies an external force acting on the fluid. The damping functions $f_{v1}$, $f_{v2}$, and $f_w$ are defined as follows:

$$f_{v1} = \frac{\chi^3}{\chi^3 + C_{v1}^3}, \quad \chi = \frac{\tilde{\nu}}{\nu}, \tag{12}$$

$$f_{v2} = 1 - \frac{\chi}{1+\chi f_{v1}}, \tag{13}$$

$$f_w = g\left[\frac{1+C_{w3}^6}{g^6 + C_{w3}^6}\right]^{\frac{1}{6}}, \tag{14}$$

where

$$g = r + C_{w2}(r^6 - r), \quad r = \frac{\tilde{\nu}}{\tilde{S}\kappa^2 d^2}. \tag{15}$$

The boundary conditions are $\mathbf{u} = \mathbf{u}_0$ at the inflow, $\mathbf{u} = \mathbf{0}$ on walls, and $p\mathbf{n} - \frac{1}{\mathrm{Re}}\nabla\mathbf{u} = \mathbf{0}$ at the outflow , where $\mathbf{n}$ the normal vector on the surface. Finally, combining Equation (8) with Equation (9),Equation (10) and Equation (11), the Lagrangian to calculate the sensitivity of the flow to geometry modifications is defined as:

$$\begin{aligned}\mathcal{L} =& \overline{C} - \frac{1}{T}\int_0^T \int_\Omega \mathbf{u}^\dagger \cdot (\frac{\partial \mathbf{u}}{\partial t} + (\mathbf{u}\cdot\nabla)\mathbf{u} + \nabla p - \nabla\cdot((\nu+\nu_t)\nabla\mathbf{u}) - \mathbf{f})\mathrm{d}\Omega\mathrm{d}t \\ & - \frac{1}{T}\int_0^T \int_\Omega p^\dagger \nabla\cdot\mathbf{u}\mathrm{d}\Omega\mathrm{d}t - \frac{1}{T}\int_0^T\int_\Omega \nu^\dagger \mathrm{SA}\mathrm{d}\Omega\mathrm{d}t,\end{aligned} \tag{16}$$

where

$$\overline{C} = -\frac{1}{T}\int_0^T \int_{\Gamma_1} (p + \frac{1}{2}\mathbf{u}^2)\mathbf{u}\cdot\mathbf{n}\mathrm{d}\Gamma\mathrm{d}t - \frac{1}{T}\int_0^T\int_{\Gamma_2}(p+\frac{1}{2}\mathbf{u}^2)\mathbf{u}\cdot\mathbf{n}\mathrm{d}\Gamma, \tag{17}$$

is the mean of the difference of total presure, SA is the transport equation of the turbulent model, $\Gamma_1$ is the inlet and $\Gamma_2$ is the outlet.

### 3.4 Sensitivity of a cost function by shape changes

The objective is to obtain an analytical formula that gives us the sensitivity to changes in geometry from which we can obtain an interpretation of the physics of the problem.

Once we have managed to calculate the sensitivity to changes in the boundary condition, we can use it to calculate the sensitivity to changes in geometry, need the following theorem [21, 22]:

Let $\Gamma_0$ the initial boundary, $(\mathbf{u}, p)$ the solution of Navier-Stokes equations, and $\Gamma'$ a perturbation on the boundary. The perturbation flow, $(\mathbf{u}', p')$ induced by the variation of the boundary satisfies the linearized Navier- Stokes's equations with the following boundary condition on the cylinder:

$$\mathbf{u}' = -\frac{\partial \mathbf{u}}{\partial \mathbf{n}}(\mathbf{v}\cdot\mathbf{n}), \tag{18}$$

where $\mathbf{v}$ is defined by $\Gamma_0 - \Gamma'$. That is, at first order, we have an identification of a perturbation in the geometry with one in the initial conditions.

If we apply this result to the sensitivity to boundary conditions, we can obtain the following expression for sensitivity to changes in geometry,

$$\nabla_\Gamma C = \langle \sigma(-p^\dagger, \mathbf{u}^\dagger)\mathbf{n}, -\frac{\partial \mathbf{u}}{\partial \mathbf{n}}\rangle\mathbf{n} + \frac{1}{a}\langle(\nu+\overline{\nu})\frac{\partial \nu^\dagger}{\partial \mathbf{n}}, \frac{\partial \overline{\nu}}{\partial \mathbf{n}}\rangle\mathbf{n}. \tag{19}$$

This equation is derived assuming that the boundary condition is now $\mathbf{g} = 0$, since we focus only on changes to the geometry of the immersed body.

Looking at the above equation, we see that the sensitivity to changes in geometry is the projection of the sensitivity to perturbation at the boundary condition on the walls onto the normal derivative of the velocity on the surface $\nabla_\Gamma C = \langle \nabla_{\mathbf{g}} C, -\frac{\partial \mathbf{u}}{\partial \mathbf{n}}\rangle\mathbf{n}$.

## 4 Preliminary Results

In the first part of the study, a laminar flow, Re = 500, within the device was chosen to validate the sensitivity equations obtained. Using Equation (19), we obtained a law that indicates the optimal way to deform the surface geometry.

In Figure 4, the sensitivity in the venturi contraction section is shown, where the need to increase the convergence angle to eliminate it.

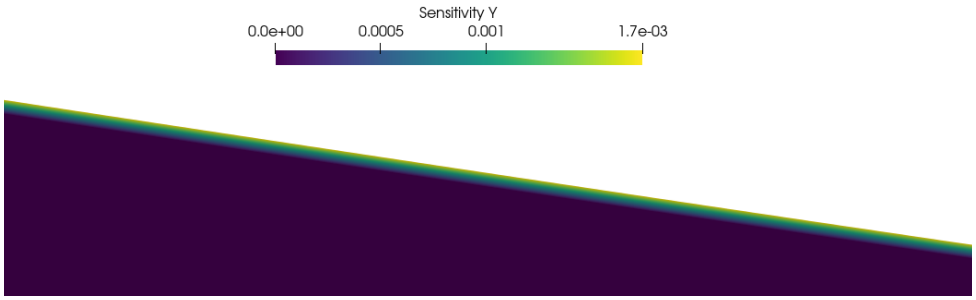


Figure 4: Sensitivity at the contraction secction.

If a perturbation in the geometry is introduced following this expression, $\Gamma = \Gamma_0 - \alpha \nabla_\Gamma C$, where $\alpha$ is a control parameter. To first order, a Taylor expansion for the cost function in terms of $\alpha$ is obtained:

$$C \sim C_0 - \alpha \langle \nabla_\Gamma C, \nabla_\Gamma C \rangle, \tag{20}$$

or equivalently

$$C - C_0 \sim -\alpha \langle \nabla_\Gamma C, \nabla_\Gamma C \rangle, \tag{21}$$

The behaviour of Equation (21) is illustrated in Figure 5, when $\alpha$ takes on low values, the numerical data closely aligns with the theoretical predictions derived from the Taylor series expansion. The difference between the theoretical value and the numerical data is only 1.2%, indicating that for small perturbations, the Taylor series provides an accurate approximation of the cost function behavior, validating the theoretical model with numerical results.

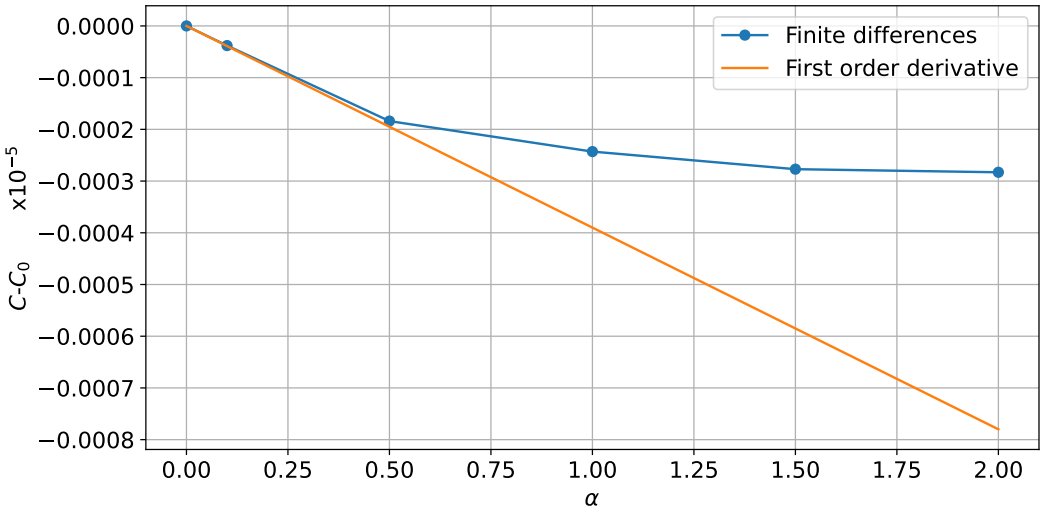


Figure 5: Pressure drop behavior in response to changes in geometry.

## 5 Conclusions

The established bijection between perturbations in shape and boundary conditions on the shape has led to a significant physical expression of sensitivity, directly linking geometric changes to boundary condition perturbations. These findings not only validate the theoretical underpinnings of our approach but also underscore its potential for broader applications. The preliminary results strongly support the effectiveness of the proposed methodology, suggesting its promise for advancing the analysis of unsteady turbulent flows. Future work will focus on refining this approach and extending its application to more complex flow scenarios, further demonstrating its versatility and impact in the field.

## REFERENCES

[1] D. de Oliveira Maionchi, L. Ainstein, F. P. dos Santos, M. B. de Souza Júnior, Computational fluid dynamics and machine learning as tools for optimization of micromixers geometry, International Journal of Heat and Mass Transfer 194 (2022) 123110.

[2] N. P. Salunke, R. J. Ahamad, S. Channiwala, S. Channiwala, Airfoil parameterization techniques: A review, American Journal of Mechanical Engineering 2 (4) (2014) 99–102.

[3] T.-C. Chiang, L.-C. Fu, Multiobjective job shop scheduling using genetic algorithm with cyclic fitness assignment, in: 2006 IEEE International Conference on Evolutionary Computation, IEEE, 2006, pp. 3266–3273.

[4] O. Pironneau, On optimum design in fluid mechanics, Journal of fluid mechanics 64 (1) (1974) 97–110.

[5] A. Jameson, Aerodynamic design via control theory, Journal of scientific computing 3 (3) (1988) 233–260.

[6] A. Jameson, Optimum aerodynamic design using cfd and control theory, in: 12th computational fluid dynamics conference, 1995, p. 1729.

[7] W. Huffman, R. Melvin, D. Young, F. Johnson, J. Bussoletti, M. Bieterman, C. Hilmes, Practical design and optimization in computational fluid dynamics, in: 23rd Fluid Dynamics, Plasmadynamics, and Lasers Conference, 1993, p. 3111.

[8] J. Elliott, J. Peraire, Practical three-dimensional aerodynamic design and optimization using unstructured meshes, AIAA journal 35 (9) (1997) 1479–1485.

[9] J. C. Newman III, A. C. Taylor III, R. W. Barnwell, P. A. Newman, G. J.-W. Hou, Overview of sensitivity analysis and shape optimization for complex aerodynamic configurations, Journal of Aircraft 36 (1) (1999) 87–96.

[10] M. B. Giles, N. A. Pierce, An introduction to the adjoint approach to design, Flow, turbulence and combustion 65 (3) (2000) 393–415.

[11] P. Meliga, E. Boujo, G. Pujals, F. Gallaire, Sensitivity of aerodynamic forces in laminar and turbulent flow past a square cylinder, Physics of Fluids 26 (10) (2014) 104101.

[12] P. Meliga, E. Boujo, M. Meldi, F. Gallaire, Revisiting the drag reduction problem using adjoint-based distributed forcing of laminar and turbulent flows over a circular cylinder, European Journal of Mechanics-B/Fluids 72 (2018) 123–134.

[13] E. J. Nielsen, B. Diskin, Discrete adjoint-based design for unsteady turbulent flows on dynamic overset unstructured grids, AIAA journal 51 (6) (2013) 1355–1373.

[14] W. Chen, C. Gao, Y. Gong, W. Zhang, Shape optimization to improve the transonic fluid-structure interaction stability by an aerodynamic unsteady adjoint method, Aerospace Science and Technology 103 (2020) 105871.

[15] A. Zymaris, D. Papadimitriou, K. Giannakoglou, C. Othmer, Continuous adjoint approach to the spalart–allmaras turbulence model for incompressible flows, Computers & Fluids 38 (8) (2009) 1528–1538.

[16] E. M. Papoutsis-Kiachagias, K. C. Giannakoglou, Continuous adjoint methods for turbulent flows, applied to shape and topology optimization: industrial applications, Archives of Computational Methods in Engineering 23 (2) (2016) 255–299.

[17] K. C. Giannakoglou, D. I. Papadimitriou, E. M. Papoutsis-Kiachagias, I. S. Kavvadias, Aerodynamic shape optimization using "turbulent" adjoint and robust design in fluid mechanics, in: Engineering and Applied Sciences Optimization: Dedicated to the Memory of Professor MG Karlaftis, Springer, 2015, pp. 289–309.

[18] I. Kavvadias, E. Papoutsis-Kiachagias, G. Dimitrakopoulos, K. Giannakoglou, The continuous adjoint approach to the k–$\omega$ sst turbulence model with applications in shape optimization, Engineering Optimization 47 (11) (2015) 1523–1542.

[19] C. J. Ruiz-Sánchez, A. Martínez-Cava, M. Chávez-Módena, E. Valero, An adjoint-based drag reduction technique for unsteady flows, Physics of Fluids 35 (7) (2023).

[20] P. Spalart, S. Allmaras, A one-equation turbulence model for aerodynamic flows, in: 30th aerospace sciences meeting and exhibit, 1992, p. 439.

[21] M. D. Gunzburger, Perspectives in flow control and optimization, SIAM, 2002.

[22] J. Sokolowski, J.-P. Zolésio, Introduction to shape optimization, in: Introduction to shape optimization, Springer, 1992, pp. 5–12.